

# The Importance of Nuclear Standards. Nuclear Metrology for Research, Applications and Impact

Patrick Henry Regan<sup>1,2,\*</sup>, Sifa Elizabeth Poulton<sup>1,2</sup>, Edward Brian O'Sullivan<sup>1,2</sup>, Steven James Bell<sup>2</sup>, Sean Michael Collins<sup>1,2</sup>, Robert Shearman<sup>2</sup>, Matthew Alan Goodwin<sup>3</sup>, and Ayrton Stewart Jenkins<sup>1,3</sup>.

<sup>1</sup>School of Mathematics and Physics, University of Surrey, Guildford, GU2 7XH, UK

<sup>2</sup>Medical, Marine and Nuclear Department, National Physical Laboratory, Teddington, TW11 0LW, UK

<sup>3</sup>AWE, Aldermaston, Reading Berkshire, RG7 4PR, UK

**Abstract.** This short conference contribution presents a review of some recent advances in radionuclide metrology at the UK's National Physical Laboratory (NPL). Particular examples include the development of novel methodologies which allow new levels of precision and measurement limits for (i) the activity and isotopic identification of radioactive gases as a proxy for real-time nuclear reactor criticality monitoring; (ii) precise ground state radioactive decay half-life determinations required for the primary standardization of pre-clinical radiopharmaceuticals and (iii) the development of a novel gamma-ray digital coincidence counting infrastructure using CeBr<sub>3</sub> fast-timing scintillation detectors. These projects generate and use precision nuclear physics data and also contribute to external studies related to specific aspects of nuclear structure physics research, including studies of nuclear pairing modes, stellar nucleosynthesis, angular momentum generation in nuclear fission and extremes of nuclear collectivity. This contribution presents a review of recent advances in radionuclide metrology at the UK's National Physical Laboratory (NPL), together with future aims and aspirations.

## 1 Introduction

The development and application of radionuclide standards for the science of precision measurement (metrology) has underpinned nuclear physics research since its inception [1]. The current frontier of radionuclide measurement relies on ongoing developments in radiation detection and digital signal processing combined with ever more precise nuclear decay data evaluations. The science of nuclear metrology contributes to a myriad of scientific disciplines enabling direct societal benefits from nuclear physics research [2] applied to key themes in the Energy & Environmental, Life Sciences & Health and Security & Resilience sectors.

The NPL Nuclear Metrology Group (NMG) undertake studies of complex nuclear decays which allow the realisation of primary and secondary radionuclide standards that are traceable to the SI unit of the becquerel (Bq) [2]. The realisation of these Bq standards has a wide range of high-impact outcomes, in particular regarding relevant measurements and calibration sources which can be used across the nuclear energy, environmental science, nuclear medicine and radiation security sectors. Recent highlights from NPL's Nuclear Metrology research portfolio include the determination of novel methodologies to provide high levels of precision and lower measurement limits for (i) radioactive gas activity concentrations (which can be as a proxy for real-time nuclear reactor criticality monitoring) [3–6]; (ii) the precision nuclear de-

cay half-life determination required for primary standardization of pre-clinical radiopharmaceuticals, in particular radium and radio-terbium isotopes [7–10]; and (iii) the ongoing development of novel coincidence measurement systems which exploit digital signal processing developments for example to provide high-precision sub-nano-second half-life measurements of excited nuclear states. In particular the NMG has developed a state-of-the-art  $\gamma$ -ray coincidence spectrometer based on LaBr<sub>3</sub>(Ce) scintillation detectors, known as the National Nuclear Array (NaNA) [11–13] which has also allowed collaboration with the wider nuclear structure and astrophysics research communities. The NPL NaNA detectors and infrastructure have contributed to a range of collaborative studies at leading international laboratories to address research questions related to: (i) nuclear isomeric decay and the spectroscopy of exotic nuclei as part of the FATIMA-DESPEC collaboration [15–19]; (ii) nucleosynthesis studies including carbon burning as part of the STELLA collaboration at the IJC Orsay France [20, 21]; (iii) measurement of extremes of quadrupole deformation close to the valence maximum and single particle structure in neutron-rich fission fragments using the NuBALL array at the IJC Facility Orsay, France [22, 23].; and (iv) for radioactive-beam resonance strength measurements linked to nuclear astrophysics studies at the TRIUMF laboratory [24]. Other recent collaborative nuclear structure physics measurements with aspects linked to NPL activity standards and data studies has included the detailed spectroscopy of the therapeutic quartet member nucleus <sup>152</sup>Tb at the ILL Greno-

\*e-mail: p.regan@surrey.ac.uk

ble facility using both high-resolution  $\gamma - \gamma$  [25] and electron- $\gamma$  coincidence studies [26] and the related precision spectroscopic study at the IFIN-HH facility, Romania to determine the B(E3) (octupole) strength in  $^{150}\text{Gd}$  following the decay of  $^{150}\text{Tb}$  [27].

The following short conference paper presents recent characterisation and development results from two key pieces of NPL radionuclide measurement infrastructure, namely the electron- $\gamma$  (PIPSBox) coincidence set-up for radioactive gas measurements and an upgrade to the NaNA digital gamma-ray coincidence infrastructure, known as NaNA plus, consisting of 20  $\text{CeBr}_3$  detectors for precision nuclear spectroscopy and nuclear decay data studies.

## 2 Gaseous Radionuclide Metrology.

In collaboration with the UK AWE, the NPL nuclear metrology group has developed a novel electron- $\gamma$  coincidence detection system for spectroscopic identification of radioactive gas species. The system allows digital coincidence detection between beta particles or discrete-energy internal conversion electrons and characteristic X-rays or discrete-energy gamma rays, which allow isotopically pure identification of decays from radioactive gases. The basic coincidence detection system developed for use at NPL is shown in Figure 1. It comprises a hyper-pure germanium (HPGe) detector system, for photon detection of characteristic decay  $\gamma$  rays and  $\text{K}_\alpha$  and  $\text{K}_\beta$  X rays, and a silicon detector (PIPSBox) for discrete-energy internal conversion electron lines and continuous-energy  $\beta$  particles [28].

The system was designed to distinguish between multiple radioactive gas species, therefore HPGe was selected for the photon detection due to its superior energy resolution. The HPGe detector used at NPL, known as *Odin*, is an ORTEC coaxial detector of diameter 93.2 mm and length 31.9 mm. The NPL-based system contained an ORTEC 120-6 pre-amplifier [28]. The electron-detection signal (from either internal conversion electrons or beta particles) was supplied by from the PIPSBox, comprising two silicon wafers with carbon fibre windows, each with a cross-sectional area of  $1200 \text{ mm}^2$  and a thickness of  $500 \mu\text{m}$ . These were positioned either side of a 10.6 mL gas volume housed within aluminium casing. Two 1/16 inch aluminium pipes with 1/8 inch VCR fittings lead into the gas volume, allowing for continuous gas flow through the detector region. For higher-activity gases, a gaseous dilution system can be added to the set up to reduce signal pile up by reducing the activity in the detection cell volume. The silicon detector output signals from the PIPSBox were connected to a CAEN A1422 preamplifier. The signals from both detectors were processed by a CAEN DT5780 MCA digitiser with a sampling rate of 500 MHz. The digitiser also supplied the voltage for the PIPSBox. For both PIPSBox and HPGe, the digitiser was set to trapezoidal rise times of  $12 \mu\text{s}$  and flat tops of  $1 \mu\text{s}$  and  $1.6 \mu\text{s}$  respectively to prioritise spectroscopy, which will have limited the count rate. Similar detection systems developed by the same collaboration are described in references [3–6].

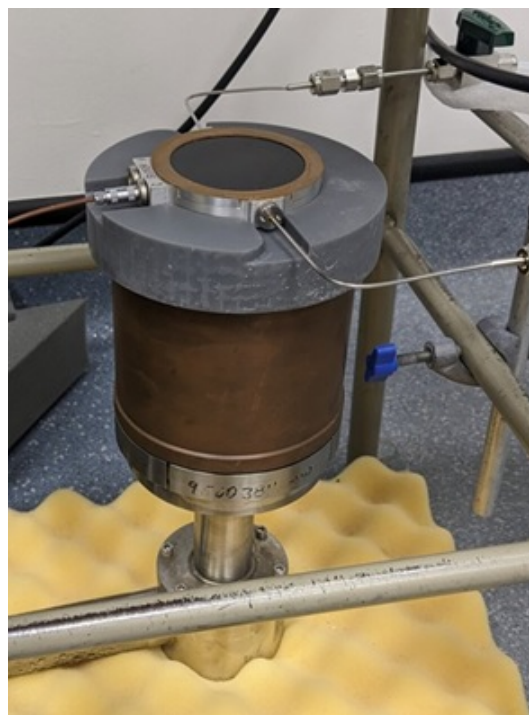


**Figure 1.** PIPSBox - HPGe system for gaseous radionuclide measurement at NPL. The (radioactive) gas input and output lines into/out of the PIPSBox can be observed in the upper part of the photograph,

A deadtime of  $25 \mu\text{s}$  was applied in data processing to reflect combined electronic limitations intrinsic to the devices. In the initial tests of the device, using a mixed  $^{131\text{m}},^{133}\text{Xe}$  calibration gas, since the digitiser used only had two independent channels, only one detector signal was taken from the two available PIPSBox silicon wafers. A CAEN A311 6 dB attenuator was used on the data cable to reduce signal size and to make it compatible with the digitiser; this also helped reduce the noise associated with the PIPSBox signal. The HPGe system was unshielded and therefore open to gamma-ray emissions from room background.

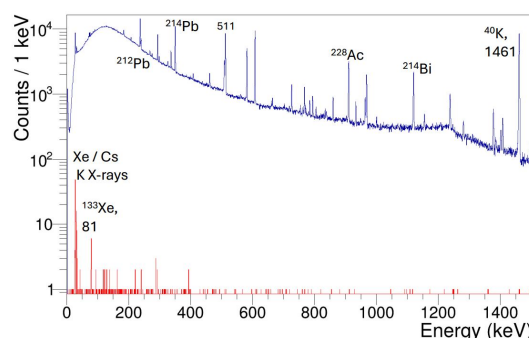


**Figure 2.** Singles and PIPSBox gated gamma-ray spectra showing the radioactive decays from  $^{131\text{m}},^{133}\text{Xe}$  calibration gas using the NPL HPGe-PIPSBox system.

**Table 1.** Table showing example gamma-ray energy signatures from typical fission fragments identified in NPL coincidence set up. Data values are taken from NNDC [29].

Parent nucleus	$T_{1/2}$ (Ground State)	Signature $E_\gamma$ (keV)
$^{87}\text{Kr}$	76.3(5) mins	403, 845, 2555
$^{88}\text{Kr}$	2.825(19) hours	196, 835, 1530
$^{133}\text{Xe}$	5.2475(5) days	79.6, 81.0
$^{135}\text{Xe}$	9.14(2) hours	250, 608
$^{138}\text{Xe}$	14.14(7) mins	258, 434, 1768, 2016
$^{138}\text{Cs}$	32.5(2) mins	463, 872, 1436, 2640

Figure 2 shows the effect of PIPSBox gating using this system with data taken from a standardised  $^{131m,133}\text{Xe}$  radioactive gas mixture tested at the NPL. The effect of placing a  $\pm 1 \mu\text{s}$  coincidence gate between events in the PIPSBox and the HPGe detector is dramatic in removing the room background lines, with only characteristic X-rays following internal conversion decay and the 81 keV gamma decay indicative of the  $^{133}\text{Xe}$  decay to  $^{133}\text{Cs}$  clearly identifiable in the gated spectrum.

A similar PIPSBox-HPGe coincidence system was setup at the AWE laboratories and used to measure airborne fission fragments and their daughter decays following the spontaneous fission of a  $^{244}\text{Cm}$  source. In this configuration, the system consisted of 2 HPGe detectors and 1 silicon detector in the PIPSBox. Table 1 lists some of the main airborne secondary fission fragment decay data observed in the AWE-based  $^{244}\text{Cm}$  measurement.

Figure 3 shows an example of data taken from this system looking at airborne fission fragments from a  $^{244}\text{Cm}$  source, measured at the AWE laboratories. The  $\gamma$ -ray singles spectra are dominated by discrete line transitions associated with decays from the primordial, naturally occurring radioactive material (NORM) background decay chains headed by  $^{238}\text{U}$  and  $^{232}\text{Th}$  and also from  $^{40}\text{K}$  (1461 keV). The addition of the  $\beta^-$  coincidence clearly pick out decays from neutron-rich fission fragments emitted from the curium source, including discrete lines indicating decays from  $^{87,88}\text{Kr}$ ,  $^{135,8}\text{Xe}$  and  $^{138}\text{Cs}$ . The gas input to the PIPS-Box was closed from the start of the AWE  $^{244}\text{Cm}$  measurements and Figure 3 shows the effect of the shorter decay half-lives for  $^{138}\text{Xe}$  ( $T_{1/2}=14.14(7)$  mins) and  $^{138}\text{Cs}$  ( $T_{1/2}=32.5(2)$  mins), compared to  $^{133,135}\text{Xe}$  ( $T_{1/2}=5.2475(5)$  days and 9.14(2) hours respectively).

### 3 Upgrade to The National Nuclear Array (NaNA)

The nuclear metrology group at NPL have developed the National Nuclear Array (NaNA) gamma-ray fast-timing digital coincidence system which has been exploited in the determination of absolute source activity and gamma-ray full-energy-peak efficiency determination [11–13]. The original NaNA design consisted of twelve 1.5 inch diameter by 2.0 inch long cerium-doped lanthanum tribromide ( $\text{LaBr}_3(\text{Ce})$ ) scintillation detectors, instrumented with a Hamamatsu R7997 photomultiplier. These were based on the FATIMA detector modules described in reference [14].

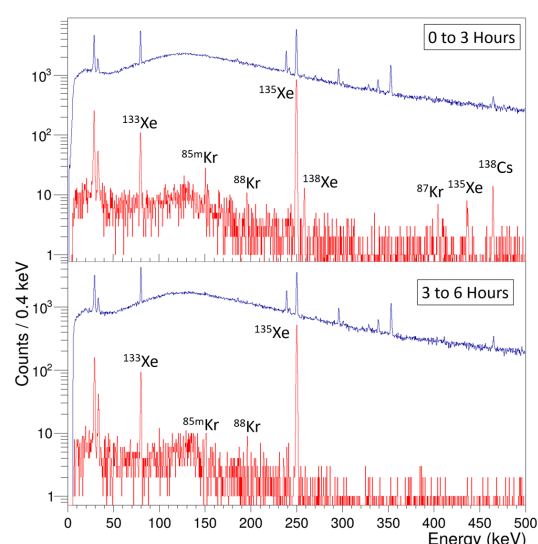


**Figure 3.** Airborne Curium-244 fission products identified using the HPGe-PIPSBox system at AWE laboratories. Note that only lines associated with the decays of  $^{133,135}\text{Xe}$  are present in the longer decay time period, with the shorter lived species of  $^{87}\text{Kr}$ ,  $^{138}\text{Xe}$  and  $^{138}\text{Cs}$  having predominantly already decayed away.

The digital processing was performed using CAEN 1 GHz 8 channel digitizers. The original NaNA infrastructure demonstrated a precise methodology for the primary standardisation of  $^{60}\text{Co}$  activity using gamma-ray singles to coincidence intensity ratios [13]. The same original NaNA detectors also enabled NPL participation in a number of collaborative research projects across the wider international nuclear structure physics research community including experimental campaigns as part of the DESPEC at GSI/FAIR Phase-0, Germany [15–19], STELLA at IJC Lab Orsay [20, 21], NuBALL at IJC Lab, France [22, 23], and the DRAGON separator at the TRIUMF laboratory, Canada [24] collaborations.

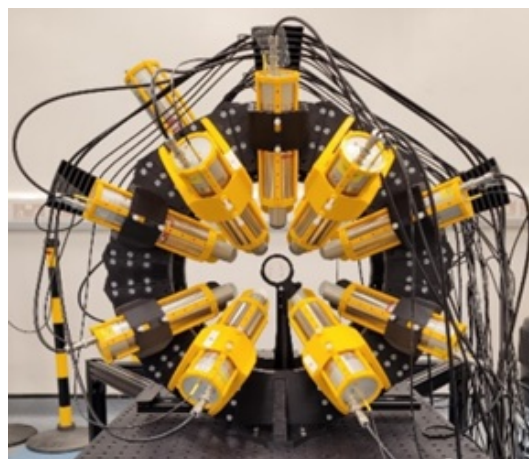


**Figure 4.** Photograph of the NaNA-plus at the National Physical Laboratory. The central ring is the source holder position.

The NaNA has recently been upgraded to a new set-up comprising twenty independent 1.0 inch diameter by 2 inch length CeBr<sub>3</sub> scintillation detectors in a more compact and better defined solid angle geometric configuration. The CeBr<sub>3</sub> scintillator crystals are coupled to Hamamatsu R13089 PMTs with built-in voltage dividers and are connected to a Caen V1751 multichannel 1 GHz digitiser. Figure 4 presents a photograph of the upgraded CeBr<sub>3</sub>-based NaNA with the central source holder position identified. The modular configuration for NaNA-plus is aided by the design of the detector holding frame which is 3-D printed and allows a range of angle and distance positions for the individual detectors to be placed in.

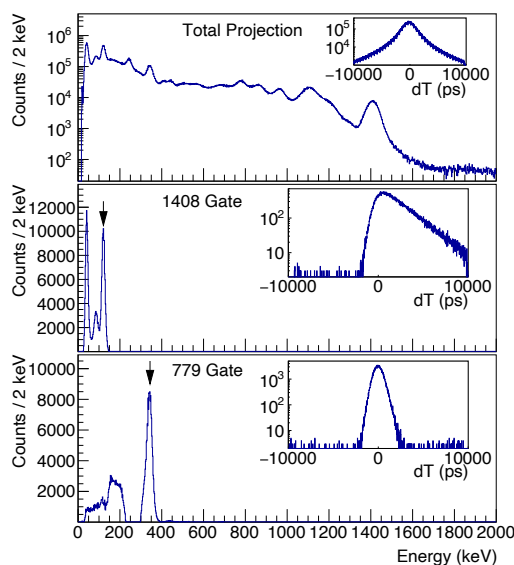


**Figure 5.** Coincidence gates on a <sup>152</sup>Eu source measurement showing the timing capabilities of the NaNA plus array for subnanosecond timing capabilities. The insets show the time differences between (upper) all gamma-ray coincidence events; (centre) the 1408 and 122 keV transitions which gate across the yrast  $I^\pi = 2^+$  state in <sup>152</sup>Sm which has an evaluated value for its half-life of 1.403(11) ns; and (lower panel) the 344 and 779 keV transitions which span across the yrast  $I^\pi = 2^+$  state in <sup>152</sup>Gd which has an evaluated half-life of 32.0(27) ps.

The basic spectral and timing performance for the upgraded NaNA configuration are demonstrated by the spectra shown in Figure 5 which shows the gamma-ray gated and total coincidence spectra measured using a standard <sup>152</sup>Eu point source, placed in the centre of the upgraded NaNA. The measured energy resolutions for the 122 and 1408 keV transitions from the <sup>152</sup>Eu source in the upgraded NaNA were approximately 16% (19 keV FWHM) and 3.5% (49 keV FWHM) respectively. The timing properties are highlighted by the  $\gamma$ -ray energy coincidence-gated time differences ( $\Delta T$ ) between the 1408 keV discrete energy gamma ray (for the decay into <sup>152</sup>Sm) and 122 keV transition and also for the time difference between the 779 keV and 344 keV transitions which are populated

in the competing source decay branch to excited states in <sup>152</sup>Gd. Both the 1408 keV and 779 keV gates directly feed into the yrast  $I^\pi = 2^+$  states in <sup>152</sup>Sm (122 keV) and <sup>152</sup>Gd (344 keV) respectively. The insets show the  $E_{\gamma 1} - E_{\gamma 2} - \Delta T$  gates which provide the measured time difference distributions between the gated coincident transitions. The central panel in Figure 5 shows the exponential slope expected for the  $T_{1/2} = 1.403(11)$  ns half-life for the  $I^\pi = 2^+$  state in <sup>152</sup>Sm which is selected using the 1408 keV and 121 keV gamma-ray energy combination [29].

## 4 Summary

This short conference paper has presented updates on experimental infrastructure based at the UK's National Physical Laboratory, specifically exploiting novel digital data acquisition techniques to allow more precise measurements of radionuclide decays, primarily using coincidence gamma-ray spectroscopy. The developments have allowed precise measurements for both airborne radioactive materials, as a signature for fission and also application in provision of state of the art nuclear decay data measurements and radionuclide standardisations using gamma coincidence spectrometry.

This work is supported by funding via a PhD scholarship bursary from the UK EPSRC. (EBOS) and a PhD Bursary provided by United Kingdom Nuclear Decommissioning Authority, managed by the UK National Nuclear Laboratory (SEP). The work performed at NPL was supported by the National Measurements System Programmes Unit of the UK's Department for Science, Innovation and Technology. PHR acknowledges support from the UK Science and Technologies Facilities Council under grant numbers ST/P005314/1, ST/V001108/1, ST/L005743/1 and ST/P005314.

## References

- [1] E. Rutherford, Radium standards and Nomenclature. *Nature* **84**, 430-431 (1910). <https://doi.org/10.1038/084430a0>
- [2] P. H. Regan et al., Radionuclide Metrology and Standards in Nuclear Physics. *Nuclear Physics News* **28(3)**, (2018). <https://doi.org/10.1080/10619127.2018.1495482>
- [3] M. A. Goodwin et al., A high-resolution  $\beta - \gamma$  coincidence spectrometry system for radionuclide measurements. *Nuclear Instruments and Methods in Physics Research A* **978**, 164452 (2020). <https://doi.org/10.1016/j.nima.2020.164452>
- [4] M. A. Goodwin et al., Production and measurement of fission product noble gases. *Journal of Environmental Radioactivity* **238-239**, 106733 (2021). <https://doi.org/10.1016/j.jenvrad.2021.106733>
- [5] M. A. Goodwin et al., Enhancing the detection sensitivity of a high-resolution  $\beta - \gamma$  coincidence spectrometer. *Journal of Environmental Radioactivity* **250**, 106915 (2022). <https://doi.org/10.1016/j.jenvrad.2022.106915>

- [6] M. A. Goodwin et al., A plastic scintillator and HPGe  $\beta$  -  $\gamma$  coincidence detection system. *Applied Radiation and Isotopes* **201**, 111028 (2023). <https://doi.org/10.1016/j.apradiso.2023.111028>
- [7] S. M. Collins et al., Half-life determination of  $^{155}\text{Tb}$  from mass-separated samples produced at CERN-MEDICIS. *Applied Radiation and Isotopes* **190**, 110480 (2022). <https://doi.org/10.1016/j.apradiso.2022.110480>
- [8] S. M. Collins et al., Determination of the Terbium-152 half-life from mass-separated samples from CERN-ISOLDE and assessment of the radionuclide purity. *Applied Radiation and Isotopes* **202**, 111044 (2023). <https://doi.org/10.1016/j.apradiso.2023.111044>
- [9] S. M. Collins et al., Determination of the  $^{161}\text{Tb}$  half-life. *Applied Radiation and Isotopes* **182**, 110140 (2022). <https://doi.org/10.1016/j.apradiso.2022.110140>
- [10] B. Webster et al., Chemical Purification of Terbium-155 from Pseudo-Isobaric Impurities in a Mass Separated Source Produced at CERN. *Scientific Reports* **9**, 10884 (2019). <https://doi.org/10.1038/s41598-019-47463-3>
- [11] G. Lorusso et al., Development of the NPL gamma-ray spectrometer NANA for traceable nuclear decay and structure studies. *Applied Radiation and Isotopes* **109**, p507-511 (2016). <https://doi.org/10.1016/j.apradiso.2015.12.050>
- [12] R. Shearman et al., Commissioning of the UK National Nuclear Array. *Radiation Physics Chemistry* **140**, p475-479 (2017). <http://dx.doi.org/10.1016/j.radphyschem.2017.02.007>
- [13] S. M. Collins et al., Investigation of  $\gamma$ - $\gamma$  coincidence counting using the National Nuclear Array (NANA) as a primary standard. *Applied Radiation and Isotopes* **134**, p290-296 (2018). <http://dx.doi.org/10.1016/j.apradiso.2017.07.056>
- [14] M. Rudigier et al., FATIMA — FAsT TIMing Array for DESPEC at FAIR, *Nuclear Instruments and Methods in Physics Research A* **969**, 163967 (2020). <https://doi.org/10.1016/j.nima.2020.163967>
- [15] A. K. Mistry et al., The DESPEC setup for GSI and FAIR. *Nuclear Instruments and Methods in Physics Research A* **1033**, 166662 (2022). <https://doi.org/10.1016/j.nima.2022.166662>
- [16] M. M. R. Chishti et al., Response of the FAsT TIMing Array (FATIMA) for DESPEC at FAIR Phase-0. *Nuclear Instruments and Methods in Physics Research A* **1056**, 168597 (2022). <https://doi.org/10.1016/j.nima.2023.168597>
- [17] A. Yaneva et al., The shape of the  $T_z = +1$  nucleus  $^{94}\text{Pd}$  and the role of proton-neutron interactions on the structure of its excited states. *Physics Letters B* **855**, 138805 (2024). <https://doi.org/10.1016/j.physletb.2024.138805>
- [18] B. Das et al., Nature of seniority symmetry breaking in the semimagic nucleus  $^{94}\text{Ru}$ . *Physical Review C* **105**, L031304 (2023). <https://doi.org/10.1103/PhysRevC.105.L031304>
- [19] E. Sahin et al., Collectivity at the prolate-oblate transition: The  $2_1^+$  lifetime of  $^{190}\text{W}$ . *Physics Letters B* **857**, 138976 (2024). <https://doi.org/10.1016/j.physletb.2024.138976>
- [20] M. Heine et al., The STELLA apparatus for particle-Gamma coincidence fusion measurements with nanosecond timing. *Nuclear Instruments and Methods in Physics Research A* **903**, p1-7 (2018). <https://doi.org/10.1016/j.nima.2018.06.058>
- [21] G. Fruet et al., Advances in the Direct Study of Carbon Burning in Massive Stars. *Physics Review Letters* **124**, 192701 (2020). <https://doi.org/10.1103/PhysRevLett.124.192701>
- [22] R. Canavan et al., Half-life measurements in  $^{164,166}\text{Dy}$  using  $\gamma$  -  $\gamma$  fast-timing spectroscopy with the  $\nu$ -Ball spectrometer. *Physical Review C* **101**, 024313 (2020). <https://doi.org/10.1103/PhysRevC.101.024313>
- [23] G. Häfner et al., Spectroscopy and lifetime measurements in  $^{134,136,138}\text{Te}$  isotopes and implications for the nuclear structure beyond  $N = 82$ . *Physical Review C* **103**, 034317 (2021). <https://doi.org/10.1103/PhysRevC.103.034317>
- [24] G. Christian et al., First in-beam demonstration of a hybrid LaBr<sub>3</sub>/CeBr<sub>3</sub>/BGO array to measure radiative capture resonance energies in an extended gas target using a novel time of flight technique. *Nuclear Instruments and Methods in Physics Research A* **1072**, 170-199 (2024). <https://doi.org/10.1016/j.nima.2024.170199>
- [25] E. B. O'Sullivan et al., Towards complete decay spectroscopy of  $^{152}\text{Tb}$ . *Radiation Physics and Chemistry* **232**, 112641 (2025). <https://doi.org/10.1016/j.radphyschem.2025.112641>
- [26] E. B. O'Sullivan et al., Electron-gamma decay spectroscopy of  $^{152}\text{Tb}$ . *Physica Scripta* **100**, 065308 (2025). <https://doi.org/10.1088/1402-4896/add812>
- [27] S. Pascu et al., Increasing Octupole Collectivity Across the  $Z=64$  Isotopic Chain:  $B(E3)$  values in  $^{150}\text{Gd}$ . *Physical Review Letters* **134**, 092501 (2025). <https://doi.org/10.1103/PhysRevLett.134.092501>
- [28] S. E. Poulton et al., Progress towards electron-photon coincidence detection of noble gases for enhanced safety monitoring of nuclear fuel. *Radiation Physics and Chemistry* **233**, 112703 (2025). <https://doi.org/10.1016/j.radphyschem.2025.112703>
- [29] National Nuclear Data Centre (NNDC). <https://www.nndc.bnl.gov/ensdf/>